Osmotic versus conventional membrane bioreactors integrated with reverse osmosis for water reuse: Biological stability, membrane fouling, and contaminant removal

Fresh manuscript submitted to ***Water Research***

November 2016

Wenhai Luo [a], Hop V. Phan [a], Ming Xie [b], Faisal I. Hai [a], William E. Price [c], Menachem Elimelech [d], Long D. Nghiem [a*]

[a] Strategic Water Infrastructure Laboratory, School of Civil, Mining and Environmental Engineering, University of Wollongong, Wollongong, NSW 2522, Australia

[b] Institute for Sustainability and Innovation, College of Engineering and Science, Victoria University, Melbourne, VIC 8001, Australia

[c] Strategic Water Infrastructure Laboratory, School of Chemistry, University of Wollongong, Wollongong, NSW 2522, Australia

[d] Department of Chemical and Environmental Engineering, Yale University, New Haven, Connecticut 06520-8286, United States

[*] Corresponding author: longn@uow.edu.au; Ph: +61 (2) 4221 4590.

Abstract

This study systematically compares the performance of osmotic membrane bioreactor – reverse osmosis (OMBR-RO) and conventional membrane bioreactor – reverse osmosis (MBR-RO) for advanced wastewater treatment and water reuse. Both systems achieved effective removal of bulk organic matter and nutrients, and almost complete removal of all 31 trace organic contaminants investigated. They both could produce high quality water suitable for recycling applications. During OMBR-RO operation, salinity build-up in the bioreactor reduced the water flux and negatively impacted the system biological treatment by altering biomass characteristics and microbial community structure. In addition, the elevated salinity also increased soluble microbial products and extracellular polymeric substances in the mixed liquor, which induced fouling of the forward osmosis (FO) membrane. Nevertheless, microbial analysis indicated that salinity stress resulted in the development of halotolerant bacteria, maintaining the OMBR system biologically active. By contrast, biological performance was relatively stable throughout conventional MBR-RO operation. Compared to conventional MBR-RO, the FO process effectively prevented foulants from permeating into the draw solution, thereby significantly reducing fouling of the downstream RO membrane in OMBR-RO operation. Accumulation of organic matter, including humic- and protein-like substances, as well as inorganic salts in the MBR effluent resulted in severe RO membrane fouling in conventional MBR-RO operation.

Keywords: Osmotic membrane bioreactor (OMBR); forward osmosis (FO); reverse osmosis (RO); trace organic contaminants (TrOCs); membrane fouling.

1. Introduction

Water scarcity due to population growth, urbanization, climate change, and environmental pollution is a vexing challenge to the sustainable development of our society (Elimelech and Phillip, 2011). This challenge calls for further efforts to develop and improve technologies that can tap into alternative water sources, such as municipal wastewater, to enhance water supply and mitigate water shortage. The ubiquitous presence of trace organic contaminants (TrOCs) in reclaimed water and wastewater-impacted water bodies remains a major obstacle to water reuse. TrOCs are emerging organic chemicals of significant concerns derived from either anthropogenic or natural activities as they present potential health risks to humans and other living organisms (Luo et al., 2014b).

Membrane bioreactor (MBR) is a well-known technology for wastewater treatment and water reuse. MBR combines conventional activated sludge (CAS) treatment and a physical membrane filtration process, typically including microfiltration (MF) and ultrafiltration (UF). As an alternative to CAS treatment, MBR is more robust and versatile and can produce higher standard effluent with smaller sludge production and physical footprint (Hai et al., 2014). Some evidence has emerged that MBR could enhance the removal of TrOCs, particularly moderately biodegradable and hydrophobic compounds compared to CAS treatment (Clara et al., 2005; De Wever et al., 2007). However, some hydrophilic TrOCs are still poorly removed by MBR due to their resistance to biodegradation and low adsorption onto sludge (Tadkaew et al., 2011; Nguyen et al., 2013; Wijekoon et al., 2013). Thus, further treatment by nanofiltration (NF) or reverse osmosis (RO) is usually required to produce high quality water for reuse (Gerrity et al., 2013). The NF/RO process can complement well MBR to achieve effective removal of various TrOCs (Alturki et al., 2010; Nguyen et al., 2013).

Recent progress in water reuse has led to the emergence of a new variation of MBR, namely, osmotic membrane bioreactor (OMBR) (Achilli et al., 2009; Cornelissen et al., 2011; Chen et al., 2014; Nguyen et al., 2016). During OMBR operation, treated water is extracted from the mixed liquor into a highly concentrated draw solution by the forward osmosis (FO) process. By employing a selective, semi-permeable FO membrane, TrOCs can be retained in the bioreactor and thus increase their biodegradation during OMBR operation (Alturki et al., 2012; Holloway et al., 2014). Moreover, FO has a lower fouling propensity, and when fouling occurs, it is readily reversible compared to pressure-driven membrane processes (Mi and Elimelech, 2010; Kim et al., 2014; Luo et al., 2015a; Xie et al., 2015).

OMBR can be used as a stand-alone process or coupled with a desalination process, such as RO to form an OMBR-RO hybrid system, for draw solution recovery and recycling water production (Luo et al., 2014a). In the latter configuration, the desalination process may provide an additional barrier to further purify the product water. For instance, Holloway et al. (2014) demonstrated that 15 of 20 TrOCs detected in municipal wastewater were removed to below detection limit by OMBR, and compounds that passed through the FO membrane were effectively retained by the subsequent RO process. An effective contaminant removal by OMBR-RO and its potential for advanced wastewater treatment and water reuse were also subsequently highlighted by Luo et al. (2016b). It is noteworthy that an MF or UF membrane was coupled with OMBR in these two studies to control salinity build-up, which is an inherent issue associated with OMBR due to the high salt rejection by the FO membrane and, more importantly, the reverse draw solute flux.

OMBR-RO can offer a range of potential benefits over conventional MBR-RO systems for advanced wastewater treatment and water reuse. Cornelissen et al. (2011) reported that OMBR-RO could reduce the capital cost of wastewater reuse by 5 – 25% compared to conventional MBR-RO using the UF membrane. Cost saving achieved by OMBR-RO

depends on the assumption that the cost and water permeability of the FO membrane are comparable to those of the UF membrane. Given the low fouling property of FO compared to UF, there can be also a reduction in operational cost related to membrane cleaning and replacement. Cornelissen et al. (2011) also assumed that the two hybrid systems had the same treatment performance, which was probably conservative as the FO membrane can produce higher quality permeate than the UF membrane. The high quality FO permeate would alleviate membrane fouling in the downstream RO process, which is a major issue for cost-effective application of conventional OMBR-RO for water reuse (Farias et al., 2014; Al Ashhab et al., 2014). Thus, additional cost saving for OMBR-RO can potentially be derived from a more stable water production from the downstream RO unit with less frequent cleaning and longer service time in comparison with conventional MBR-RO. Of a particular note, to date, no study has directly compared the performance of OMBR-RO and conventional MBR-RO for water reuse.

This study aims to compare the performance of OMBR-RO with conventional MBR-RO in terms of biological stability, contaminant removal, and membrane fouling. Similar operating parameters were applied to both bioreactors for a systematic comparison. Water production and salinity build-up during OMBR-RO operation were evaluated. High-throughput sequencing technique was applied to elucidate the effect of salinity build-up on microbial community structure during OMBR-RO operation compared to that in conventional MBR-RO. Fate and transport behaviours of bulk organic matter, nutrients, and TrOCs in these two hybrid systems were systematically examined. In addition, the fouling behaviour of the RO membrane in both systems was also delineated and compared.

2. Materials and methods

2.1 Synthetic wastewater and trace organic contaminants

A synthetic wastewater was used in this study. The synthetic wastewater was prepared daily to obtain 100 mg/L glucose, 100 mg/L peptone, 17.5 mg/L KH_2PO_4, 17.5 mg/L $MgSO_4$, 10 mg/L $FeSO_4$, 225 mg/L CH_3COONa, and 35 mg/L urea (Alturki et al., 2010).

A set of 31 TrOCs were selected to represent four major groups of emerging organic chemicals of significant concern — endocrine disrupting compounds, pharmaceutical and personal care products, industrial chemicals, and pesticides — that occur ubiquitously in municipal wastewater. Key physicochemical properties of these TrOCs are summarized in Table S1, Supplementary Data. Based on their effective octanol – water partition coefficient (i.e. Log D) at solution pH 8, the 31 TrOCs could be categorized as hydrophobic (i.e. Log D > 3.2) and hydrophilic (i.e. Log D < 3.2) (Tadkaew et al., 2011). A stock solution containing 25 µg/mL of each of TrOCs was prepared in pure methanol and stored at -18 °C in the dark. The stock solution was introduced into the synthetic wastewater described above to obtain a concentration of 5 µg/L of each compound. The TrOC stock solution was used within a month.

2.2 Experimental systems

2.2.1 Osmotic membrane bioreactor – reverse osmosis

A lab-scale OMBR-RO system was used (Figure S1a, Supplementary Data). This hybrid system was consisted of a feed solution reservoir, a glass bioreactor with a submerged, plate-and-frame FO membrane cell, a draw solution reservoir, and a cross-flow RO unit. A water level controller was used to regulate a Masterflex peristaltic pump (Cole-Parmer, Vernon Hills, IL) to feed the bioreactor. The feed reservoir was positioned on a digital balance

(Mettler-Toledo, Hightstown, IL), which was connected to a computer. A decrease in the feed reservoir weight was recorded and then used to calculate the FO water flux.

The FO membrane cell was made of acrylic plastic. A flat-sheet, thin-film composite (TFC) FO membrane was mounted on the cell to seal the draw solution flow channel of 20 cm long, 15 cm wide, and 0.4 cm high. The membrane active layer was in contact with the mixed liquor (i.e. FO mode) with an effective surface area of 300 cm^2. The draw solution was circulated from a stainless steel reservoir to the membrane cell by a gear pump (Micropump, Vancouver, WA) at a cross-flow velocity of 2.8 cm/s.

The TFC FO membrane used in this study was obtained from Hydration Technology Innovations (Albany, OR). Similar to TFC FO membranes from other suppliers (e.g. Oasys Water and Porifera), this membrane comprised a thin, selective polyamide active layer and a porous polysulfone support layer. These TFC FO membranes have higher rejection capacity and much higher water permeability than cellulose triacetate based FO membranes (Cath et al., 2013). In fact, TFC FO membranes with two to three times higher water permeability than the membrane used in this study have been recently reported (Tian et al., 2015; Wei et al., 2015). It is noted that the polyamide active layer of commercial membranes can be slightly modified by proprietary additives. In addition, the support layer structure can also influence the membrane water permeability (Lu et al., 2015). However, this study was specific to the comparison between OMBR and conventional MBR, rather than membrane properties. Thus, findings from this study are still valid to OMBR using other FO membranes.

The cross-flow RO unit, comprising a Hydra-Cell high pressure pump (Wanner Engineering, Minneapolis, MN) and a membrane cell made of stainless steel, was coupled with OMBR to reconcentrate the draw solution and produce recycling water. A flat-sheet, TFC polyamide RO membrane (LFC3, Hydranautics, Oceanside, CA) was embedded into the membrane cell

with a flow channel height of 0.2 cm and an effective membrane surface area of 40 cm^2 (4 cm × 10 cm). A bypass valve and a back-pressure regulator (Swagelok, Solon, OH) were used to adjust the hydraulic pressure and cross-flow velocity. A temperature controller (Neslab RTE7, Waltham, MA) installed with a stainless steel heat exchanger coil was used to maintain the RO feed (i.e. OMBR draw solution) temperature at 21 ± 1 °C. Water flux was monitored by a digital flow meter (Optiflow, Palo Alto, CA), which was connected to a computer. Key properties of the FO and RO membranes used in the OMBR-RO hybrid system are provided in Table S2, Supplementary Data.

2.2.2 Conventional membrane bioreactor – reverse osmosis

A lab-scale, conventional MBR-RO system was composed of a hollow fibre MF membrane module (Mitsubishi Rayon Engineering, Tokyo, Japan) in a glass bioreactor and an RO unit (Figure S1b, Supplementary Data). The bioreactor and RO unit were identical to those used in the OMBR-RO system. The MF membrane was made of polyvinylidene fluoride with a nominal pore size and an effective surface area of 0.4 μm and 740 cm^2, respectively. The MF membrane driven by a Masterflex peristaltic pump (Cole-Parmer, Vernon Hills, IL) was operated in a cycle of 14 min suction and 1 min relaxation. The relaxation time was set to reduce membrane fouling. A high resolution (±0.1 kPa) pressure sensor (Extech Equipment, Australia) was installed to record the trans-membrane pressure (TMP).

2.3 Experimental protocol

Activated sludge from the Wollongong Wastewater Treatment Plant (Wollongong, Australia) was used to inoculate the two bioreactors. The bioreactors were acclimatized to the synthetic wastewater described above for over 60 days using MF membranes for effluent extraction under the same conditions. Once acclimatized with regards to bulk organic removal (i.e. over 97% total organic carbon (TOC) removal), the MF membrane was removed from one

bioreactor, which was then integrated with the FO and RO components to form the OMBR-RO hybrid system. A same RO component was coupled with the other bioreactor to establish the conventional MBR-RO system.

Both OMBR-RO and conventional MBR-RO systems were continuously operated for 40 days under similar conditions in a constant temperature room (22 ± 1 °C). The bioreactors with working volume of 6 L were continuously aerated to obtain a mixed liquor dissolved oxygen (DO) concentration of 5 ± 1 mg/L. The initial mixed liquor suspended solids (MLSS) concentration was adjusted to approximately 5 g/L. The sludge retention time (SRT) was controlled at 20 days by daily wasting 300 mL mixed liquor. The hydraulic retention time (HRT) was in the range of 27 – 60 hours determined by the water flux of OMBR. A 0.5 M NaCl draw solution (with effective volume of 10 L) was used for OMBR. On day 20, 100 g NaCl was added to replenish draw solute loss caused by the reverse salt flux and its passage through the downstream RO membrane. This amount was calculated based on a decrease in the electrical conductivity of the draw solution and a NaCl calibration curve.

Water flux of the conventional MBR was adjusted daily to be equal to that of OMBR to systematically compare their effects on the downstream RO process. At the same time, the RO water flux was also adjusted accordingly by regulating the applied hydraulic pressure while fixing the cross-flow velocity at 41.7 cm/s. As a result, the working volume of the draw solution and MBR effluent was constant at 10 L over the entire experimental period. No membrane cleaning was conducted for both systems during their operation. A new RO membrane was used once its normalized water permeability decreased to 0.2.

198 *2.4 Analytical methods*

199 *2.4.1 Measurement of basic water quality parameters*

200 Basic water quality parameters were analysed every three days. Specifically, TOC and total
201 nitrogen (TN) were analysed using a TOC/TN analyser (TOC-V_{CSH}, Shimadzu, Kyoto).
202 Ammonium (NH_4^+) and orthophosphate (PO_4^{3-}) were determined by a Flow Injection
203 Analysis system (QuikChem 8500, Lachat, CO). An Orion 4-Star Plus pH/conductivity meter
204 (Thermo Scientific, Waltham, MA) was used to monitor the solution pH and electrical
205 conductivity on a daily basis.

206 *2.4.2 Measurement of trace organic contaminants*

207 Aqueous samples were taken from the OMBR-RO and MBR-RO systems every ten days for
208 TrOC analysis using a method previously described by Hai et al. (2011). Briefly, the method
209 involved solid phase extraction, derivatisation, and quantification by a gas chromatography –
210 mass spectrometry system (QP5000 GC-MS, Shimadzu, Kyoto).

211 In OMBR-RO, TrOC removal rates by the bioreactor (R_{Bio}), OMBR (R_{OMBR}), and OMBR-RO
212 ($R_{Overall}$) are defined as follows:

213 $$R_{Bio} = (1 - \frac{C_{Sup}V_{Bio} + C^*_{Draw}\Delta V_{FO}}{C_{Feed}\Delta V}) \times 100\% \quad (1)$$

214 $$R_{OMBR} = (1 - \frac{C^*_{Draw}}{C_{Feed}}) \times 100\% \quad (2)$$

215 $$R_{Overall} = (1 - \frac{C_{Permeate}}{C_{Feed}}) \times 100\% \quad (3)$$

216 where C_{Feed}, C_{Sup}, and $C_{Permeate}$ is the measured TrOC concentration (ng/L) in the feed, mixed
217 liquor supernatant, and RO permeate, respectively; C^*_{Draw} is the TrOC concentration in the
218 FO permeate; V_{Bio} is the effective bioreactor volume (i.e. 6 L); and ΔV_{FO} is the volume of

water passed through the FO membrane between time t and $t+\Delta t$. TrOCs accumulate in the draw solution when they pass through the FO membrane but are retained by the subsequent RO membrane (D'Haese et al., 2013). Thus, C^*_{Draw} is determined from a mass balance:

$$C^*_{Draw} = \frac{M_{FO}}{Q_{FO}} \quad (4)$$

$$M_{FO} = \frac{V_{Draw}(C_{Draw(t+\Delta t)} - C_{Draw(t)})}{\Delta t} + \frac{\frac{(C_{RO(t+\Delta t)} + C_{RO(t)})}{2}\Delta V}{\Delta t} \quad (5)$$

$$\Delta V = Q_{RO}\Delta t \quad (6)$$

where M_{FO} is the mass flow rate of TrOCs crossed through the FO membrane; $C_{Draw(t)}$ and $C_{Draw(t+\Delta t)}$ is the measured TrOC concentration in the draw solution at time t and $t+\Delta t$, respectively; $C_{RO(t)}$ and $C_{RO(t+\Delta t)}$ is the measured TrOC concentration in the RO permeate at time t and $t+\Delta t$, respectively; and Q_{FO} and Q_{RO} is the water flux of the FO and RO membranes, respectively. As noted in Section 2.3, the RO water flux (Q_{RO}) was adjusted to be equal to that of the FO membrane (Q_{FO}). Based on eqs. (4) – (6), C^*_{Draw} is calculated from

$$C^*_{Draw} = \frac{V_{Draw}(C_{Draw(t+\Delta t)} - C_{Draw(t)})}{\Delta V_{FO}} + \frac{(C_{RO(t+\Delta t)} + C_{RO(t)})}{2} \quad (7)$$

According to eqs. (1) – (3), the observed TrOC rejection rate by the FO ($R_{Ob\,FO}$) and RO ($R_{Ob\,RO}$) membranes is calculated as:

$$R_{ObFO} = R_{OMBR} - R_{Bio} \quad (8)$$

$$R_{ObRO} = R_{Overall} - R_{OMBR} \quad (9)$$

The observed TrOC rejection rate does not reflect the real separation capacity of the FO and RO membranes, but can be used to infer their contributions to TrOC removal in OMBR-RO. Similar to OMBR-RO operation, the RO water flux was adjusted daily to match the MBR

effluent flow rate, maintaining the effluent reservoir with a working volume of 10 L during conventional MBR-RO operation (Section 2.3). Therefore, the calculation process listed above was also applicable to evaluate TrOC removal by different compartments of conventional MBR-RO.

2.4.3 Fluorescence excitation – emission matrix spectroscopy

Fluorescence intensities of the OMBR and MBR mixed liquor supernatant, draw solution, and MBR effluent samples at the beginning and conclusion of OMBR-RO and conventional MBR-RO operation were measured to determine organic substances likely responsible for fouling of the RO membrane using a two-dimensional fluorescence spectrophotometer (Perkin-Elmer LS-55) with excitation wavelengths between 240 and 450 nm and emission wavelengths between 290 and 580 nm (in 5 nm increments). Samples were prepared and analysed based on the method reported by Cory and McKnight (2005). Fluorophores detected in certain areas of optical space in an excitation-emission-intensity matrix (EEM) correspond to specific fractions of dissolved organic matter (Henderson et al., 2009; Xie and Gray, 2016). All samples were diluted to a same TOC concentration for resolving and comparing EEM spectra.

2.4.4 Microbial community analysis

Sludge samples were taken at the beginning and conclusion of OMBR and conventional MBR operation for microbial community analysis according to a method reported previously by Luo et al. (2016c). In brief, the method included DNA extraction using the FastDNA® SPIN Kit for soil (MP Biomedicals, Santa Ana, CA), PCR amplification of V1 – V3 16S rRNA gene, and amplicon sequencing on a Illumina MiSeq platform (Australian Genome Research Facility, Queensland, Australia).

Paired-end reads were assembled using PEAR (version 0.9.8) (Zhang et al., 2014) and then processed with Quantitative Insights into Microbial Ecology (QIIME 1.9.1) (Caporaso et al., 2010), USEARCH (version 8.0.1623) (Edgar, 2013), and UPARSE pipeline. All sequencing data here are available at the Sequence Read Archive (accession number: SRP072961) in the National Centre for Biotechnology Information (Bethesda, MD).

2.4.5 Biomass characterisation

MLSS and mixed liquor volatile suspended solids (MLVSS) concentrations in the bioreactor were analysed based on Standard Method 2540 (APHA, 2005). Biomass activity was evaluated by determining the specific oxygen uptake rate (SOUR) of activated sludge using Standard Method 1683 (APHA, 2005). Extracellular polymeric substance (EPS) in the sludge were extracted using a method from Zhang et al. (1999). EPS and soluble microbial products (SMP) in the mixed liquor were measured by analysing their protein and polysaccharide concentrations. Proteins and polysaccharides were determined by the Folin method with bovine serum albumin as the standard and the phenol-sulfuric acid method with glucose as the standard, respectively (Semblante et al., 2015).

2.4.6 Membrane autopsy

At the conclusion of OMBR-RO and conventional MBR-RO operation, a scanning electron microscopy (SEM) coupled with energy dispersive spectroscopy (EDS) (JCM-6000, JEOL, Tokyo, Japan) was used to identify the morphology and composition of the fouling layer on the membrane surface. Membrane samples were air-dried in a desiccator before being coated with an ultra-thin gold layer with a sputter coater (SPI Module, West Chester, PA) for SEM imaging. Attenuated Total Reflection – Fourier Transform Infrared (ATR-FTIR) spectroscopy (IRAffinity-1, Shimadzu, Kyoto, Japan) was also used to probe the chemical composition of the fouling layer. The measured spectrum ranged between 600 and 4000 cm^{-1}

with 2 cm^{-1} resolution. Each scan was performed 20 times. A background correction was conducted before each measurement.

3. Results and discussion

3.1 Process performance

3.1.1 Mixed liquor salinity and water flux

Salinity build-up in the bioreactor is an inherent issue associated with OMBR due to the effective salt rejection by the FO membrane and the reverse draw solute flux. Thus, the mixed liquor conductivity increased significantly within the first 10 days of OMBR operation (Figure 1). Less significant conductivity increase was observed thereafter, which could be attributed to a decrease in the reverse draw solute flux associated with the water flux decline. At the same time, daily sludge wastage to control the SRT could also remove some dissolved inorganic salts, contributing to a more gradual conductivity increase from day 10 onward (Figure 1). High salinity could negatively affect the system biological stability and membrane performance (Lay et al., 2010). Since salinity build-up continued to occur, a long term study is necessary to determine the steady state level of salinity in the bioreactor. It is also noted that several strategies to mitigate salinity build-up in OMBR have been proposed, for example, by using organic draw solutions (Luo et al., 2016a) and integrating with the MF/UF membrane for salt bleeding (Holloway et al., 2015; Luo et al., 2016b).

In contrast to salinity build-up in OMBR, the mixed liquor conductivity was constant at approximately 0.38 mS/cm (corresponding to 0.19 g/L NaCl) throughout conventional MBR operation (Figure 1). This is because the MF membrane does not retain any dissolved salts. Overall, different sludge characteristics, microbial community structure, and biological treatment performance between OMBR and conventional MBR were observed as discussed in the following sections.

[Figure 1]

A continuous decrease in the water flux was observed for OMBR (Figure 1). The observed flux decline could be ascribed to salinity build-up in the bioreactor, a decrease in the draw solution concentration, and membrane fouling. Although the RO membrane effectively rejected NaCl solute (> 98%), the draw solution concentration decreased over time (Figure S2, Supplementary Data), due to the reverse solute transport and, to a lesser extent, its passage through the RO membrane. Both salinity increase in the bioreactor and concentration decrease of the draw solution could reduce the net driving force (i.e. effective trans-membrane osmotic pressure) for water permeation. On day 20 of the experiment, 100 g NaCl was added to replenish the draw solute loss, which slightly enhanced the water flux (by approximately 1.5 L/m^2h). Despite the low fouling propensity of the FO membrane, a cake layer was observed on the membrane surface at the conclusion of OMBR operation, predominately consisting of carbon, oxygen, phosphorus, sodium, magnesium, and calcium (Figure S3, Supplementary Data).

Water flux of conventional MBR was adjusted daily to match that of OMBR and thus maintain a comparable effluent flux toward the downstream RO process. As a result, the MF membrane was operated at a relatively low water flux, which in turn resulted in negligible membrane fouling as indicated by a small TMP increase throughout conventional MBR operation (Figure S4, Supplementary Data). In practice, the water flux of conventional MBR is usually above 10 L/m^2h (Hai et al., 2014), which is considerably higher than the water flux (4 – 8 L/m^2h) used in this study. Although FO is more resistant to fouling compared to UF/MF given the different mechanisms of water transport (i.e. osmotically driven and hydraulic pressure driven for FO and UF/MF, respectively), fouling behaviour and separation performance of FO at a higher flux can differ from those reported here. Nevertheless, with continued progress in membrane development (Fane et al., 2015; Shaffer et al., 2015; Werber

et al., 2016), fouling resistant, high flux and high separation performance FO membranes can be available in a near future. Indeed, several different research groups have reported new FO membranes with water permeability two to three times higher than that of the commercial membrane used in this study (Tian et al., 2015; Wei et al., 2015). Such progress in membrane fabrication may provide more opportunities in the deployment of OMBR with better contaminant removal and less membrane fouling.

3.1.2 Biomass characteristics

Salinity build-up in the bioreactor altered biomass characteristics during OMBR operation (Figure 2). A small but discernible decrease in biomass concentration (i.e. MLSS and MLVSS) and SOUR was observed within the first two weeks (Figure 2a-c). This observation is in good agreement with previous studies (Wang et al., 2014; Luo et al., 2015b), and could be ascribed to the inhibition on biomass growth and activity with salinity increase. In addition, the high salinity also increased SMP and EPS concentrations in the mixed liquor (Figure 2d, e), which might be responsible for the FO membrane fouling as discussed above. It has been reported that the elevated salinity could increase the endogenous respiration of microorganisms in activated sludge and thus enhance the secretion of organic cellular substances (Lay et al., 2010; Chen et al., 2014). Nevertheless, biomass concentration and activity recovered gradually from day 14 onward, possibly due to microbial acclimatization to the saline condition, which consequently resulted in the dominance of halotolerant bacteria in the bioreactor (Figures 3 and 4). Meanwhile, SMP and EPS concentrations in the mixed liquor decreased and then stabilized at approximately 20 and 55 mg/g MLVSS, respectively (Figure 2d, e).

[Figure 2]

Biomass growth (indicated by the MLSS and MLVSS concentrations) and activity (indicated by the sludge SOUR) were relatively stable during conventional MBR operation (Figure 2). However, both SMP and EPS concentrations in the mixed liquor decreased significantly, likely due to a reduction in the organic loading rate caused by the decreasing water flux (to match that of OMBR). Given a stable sludge concentration, a decrease in the organic loading rate could lower the ratio of food to microorganism (i.e. F/M), thereby increasing the SMP and EPS biodegradation (Wu et al., 2013).

3.1.3 Microbial community structure

Sludge samples collected from OMBR and conventional MBR were clustered based on the unweighted Unifrac distance by applying hierarchical clustering (Figure 3). The unweighted Unifrac distance among samples represents the dissimilarity in their microbial communities in a phylogenetic tree. Results show that microbial community structure varied differently in OMBR and conventional MBR (Figures 3 and 4). Sludge samples taken at the beginning of OMBR and conventional MBR operation (i.e. on day 0) formed one cluster, confirming similar microbial communities in these two systems at the initial phase (Figure 3). However, the sludge sample collected at the end of OMBR operation (i.e. on day 40) created a branch distinct from the cluster of other samples. This result indicates that salinity build-up in OMBR significantly impacted the development of the microbial community, rendering it different from that in conventional MBR. In addition, distant clusters were observed for the two sludge samples taken at the beginning and conclusion of conventional MBR operation. This observation could be attributed to microbial variation in response to the prolonging HRT due to continuous water flux decline (Figure 1). It is noteworthy that natural and transient changes in microbial community during MBR operation could also occur (Luo et al., 2016c; Phan et al., 2016).

[Figure 3]

[Figure 4]

Further taxonomic analysis revealed significant difference in the microbial community between OMBR and conventional MBR (Figure 3). For instance, the phylum *Planctomycetes* in conventional MBR was much more abundant than that in OMBR (Figure 4a). This result is consistent with our previous study that showed a decrease in the abundance of the phylum *Planctomycetes* in a conventional MBR when its influent salinity increased (Luo et al., 2016c). Microbial species of the phylum *Bacteroidetes* are usually detected in both marine and freshwater environments (Zhang et al., 2013). Thus, the phylum *Bacteroidetes* was identified in all sludge samples with noticeable abundance (Figure 4a). Nevertheless, the abundance of the phylum *Bacteroidetes* increased during OMBR operation, which could be further attributed to an increase in the dominance of the family *Cytophagaceae* (Figure 4b).

Abundance of the phylum *Proteobacteria* varied differently during OMBR and conventional MBR operation, although it was the most abundant phylum in both systems (Figure 4a). As conventional MBR operated, the abundance of the phylum *Proteobacteria* increased significantly, which was mainly contributed by the dominance of the class *β-proteobacteria*. Members of the class *β-proteobacteria* are typically dominant in freshwater environment (Zhang et al., 2013). Detailed analysis attributed this class dominance to the predominance of the families *Oxalobacteraceae* and *Comamonadaceae* (Figure 4b). By contrast, a small increase in the abundance of the class *β-proteobacteria* was observed during OMBR operation, which was only contributed by the dominance of the family *Comamonadaceae*. Zhang et al. (2013) also reported an increase in the abundance of the class *β-proteobacteria* along a salinity gradient of 0.34 – 6.86 g/L NaCl in a Chinese wetland. These results indicate that some microbes affiliated to the class *β-proteobacteria*, such as *Comamonadaceae*, are salt-tolerant and could proliferate under saline conditions. On the other hand, the abundance of the class *γ-proteobacteria* decreased considerably in both systems mainly due to the

decaying of the family *Xanthomonadaceae*. A similar decrease in both systems also occurred for the family *Ellin 6075* belonged to the phylum *Acidobacteria*.

3.2 Contaminant removal

3.2.1 Removal of bulk organic matter and nutrients

No significant difference between OMBR-RO and conventional MBR-RO was observed regarding overall removal of bulk organic matter (i.e. TOC and TN) (Figure 5) and nutrients (i.e. NH_4^+ and PO_4^{3-}) (Figure 6). Nevertheless, these contaminants exhibited considerably different fates and transport behaviours in the two hybrid systems. A small increase in TOC concentration in the bioreactor was observed at the beginning of OMBR operation (Figure 5a). This observation could be attributed to negative effects of salinity build-up on biomass activity as discussed above and the high rejection of biologically persistent substances by the FO membrane. The high rejection FO membrane resulted in negligible TOC concentration in the draw solution and thus ensured a complete overall removal by OMBR-RO. Given the stable biological treatment and the permeation of non-biodegradable organic substances through the MF membrane, TOC concentration in the bioreactor during conventional MBR operation was less than one-tenth of that in OMBR (Figure 5b). Organic substances that were resistant to conventional MBR treatment were effectively retained by the RO membrane, causing notable TOC accumulation in the MBR effluent reservoir and near complete removal by the whole system.

[Figure 5]

Without a denitrification step, TN removal by activated sludge is limited and depends mainly on microbial assimilation (Hai et al., 2014). In OMBR-RO operation, the high rejection FO and RO membranes induced a considerable TN accumulation in the bioreactor and the draw solution, respectively (Figure 5c). It has been reported that contaminants that permeated

through the FO membrane but were rejected by the RO membrane could accumulate in the draw solution in closed-loop FO-RO systems (e.g. OMBR-RO), and eventually deteriorated the product water quality (Shaffer et al., 2012; D'Haese et al., 2013). As a result, the overall TN removal by OMBR-RO decreased from nearly 100 to 50% within 40 days (Figure 5c). By contrast, TN concentration in the bioreactor was stable at approximately 30 mg/L during conventional MBR operation (Figure 5d). Nevertheless, the high rejection RO membrane caused a significant TN build-up in the MBR effluent reservoir, which consequently reduced its overall removal by MBR-RO (from approximately 98 to 40%).

Effective nitrification occurred in both OMBR and conventional MBR systems as manifested by the removal of NH_4^+ in their bioreactors (Figure 6a, b). Nevertheless, ammonia oxidizing bacteria (AOB), which oxidize ammonia to nitrite, were not efficiently detected in all sludge samples (Figure 4). Only nitrite oxidizing bacteria (which oxidize nitrite to nitrate) affiliated to the phylum *Nitrospirae* were identified at a small abundance (Figure 4a). Similar results were also reported previously and could be attributed to the presence of AOB species that were unidentifiable by 16S rRNA-gene sequencing (Luo et al., 2016c; Phan et al., 2016). Additionally, the effective NH_4^+ removal could also be contributed by ammonia oxidizing archaea, which however, were not targeted by the primers designed in this study.

[Figure 6]

Similar to bulk organic matter (i.e. TOC), a small and transient increase in NH_4^+ concentration was observed in the bioreactor at the beginning of OMBR operation (Figure 6a). Nevertheless, the high rejection FO membrane resulted in negligible NH_4^+ concentration in the draw solution. On the other hand, NH_4^+ concentration in the bioreactor was constantly low during conventional MBR operation. However, the high rejection RO membrane induced a small but discernible NH_4^+ build-up in the MBR effluent reservoir from day 20 onward.

Without chemical precipitation, phosphate removal in activated sludge treatment relies mainly on microbial assimilation, especially by polyphosphate accumulating organisms (PAOs). PAOs are vulnerable to saline stress and a small osmotic pressure increase within their cells caused by salinity build-up may severely reduce their phosphate accumulating ability (Lay et al., 2010; Yogalakshmi, 2010). Nevertheless, the FO membrane can almost completely retain phosphate ions as they are negatively charged and have large hydrated radius (Holloway et al., 2007). As a result, PO_4^{3-} accumulated considerably in the bioreactor while its presence in the draw solution was negligible during OMBR-RO operation (Figure 6c). On the other hand, phosphate could permeate through the MF but not the RO membrane. Thus, phosphate build-up in the MBR effluent reservoir was observed during conventional MBR-RO operation (Figure 6d). It is noteworthy that PO_4^{3-} concentration in the bioreactor was slightly higher than that in influent during conventional MBR operation, possibly owing to its retention by the dynamic fouling layer formed on the MF membrane surface and/or phosphate release from unmetabolized substrates (Yogalakshmi, 2010).

3.2.2 Removal of trace organic contaminants

All 31 TrOCs investigated were almost completely removed by both OMBR-RO and conventional MBR-RO (Figure 6), due to the synergy of biological treatment and physical membrane rejection. Nevertheless, removal behaviours of these TrOCs were significantly different in these two hybrid systems, depending on their physiochemical properties, including hydrophobicity and molecular structure (Table S1, Supplementary Data). Of the 31 TrOCs investigated, 18 compounds were hydrophilic (i.e. Log D < 3.2) and 13 compounds were hydrophobic (i.e. Log D > 3.2) (Section 2.1).

[Figure 7]

All 13 hydrophobic TrOCs were biologically removed by over 90% in both systems (Figure 7). Compared to conventional MBR, salinity build-up in the bioreactor did not significantly affect the biological removal of these hydrophobic compounds during OMBR operation. Their high removal by activated sludge has also been demonstrated in several previous studies (Tadkaew et al., 2011; Wijekoon et al., 2013) and can be ascribed to their adsorption onto sludge, which facilitated their biodegradation. Results reported here are also consistent with a previous study by Luo et al. (2015b) who reported insignificant variation in the removal of hydrophobic TrOCs by conventional MBR as the mixed liquor salinity increased (up to 16.5 g/L NaCl). The effective removal of hydrophobic TrOCs by activated sludge could consequently reduce their permeation through the FO and subsequent RO membranes, leading to near complete removal by both hybrid systems (Figure 7). It has been reported that an initial adsorption but subsequent partition and diffusion of hydrophobic TrOCs (particularly, non-ionic compounds) through membranes could reduce their rejection in a stand-alone FO or RO process (Nghiem and Coleman, 2008; Xie et al., 2014).

Varying removal rates of hydrophilic TrOCs were observed in both bioreactors (Figure 7). Effective removal (> 90%) was observed for several hydrophilic compounds, including salicylic acid, ketoprofen, naproxen, metronidazole, ibuprofen, gemfibrozil, enterolactone, pentachlorophenol, DEET, and estriol. This result can be attributed to the high biodegradability of these compounds, whose molecular structures have strong electron donating functional groups (e.g. amine and hydroxyl) (Tadkaew et al., 2011). On the other hand, some hydrophilic TrOCs were poorly removed in both bioreactors, with removal rates only in the range of 20 – 70%. They included clofibric acid, fenoprop, primidone, diclofenac, carbamazepine, atrazine, and ametryn, which are well-known biologically resistant substrates. Their resistance to biological treatment mainly resulted from the presence of strong electron withdrawing functional groups (such as chloride, amide, and nitro) or the lack

of strong electron donating functional groups in their molecular structures (Tadkaew et al., 2011; Wijekoon et al., 2013).

Despite the low removal of biologically persistent TrOCs by activated sludge, the high rejection FO membrane prevented their permeation into the draw solution and allowed almost complete removal by OMBR (Figure 7a). A small but nevertheless discernible contribution by the downstream RO membrane was only observed for atrazine and ametryn, which were slightly permeable through the FO membrane. Our results are consistent with previous studies which demonstrated excellent removal of TrOCs by FO or FO-RO (Hancock et al., 2011; D'Haese et al., 2013; Alturki et al., 2013). On the other hand, conventional MBR could not effectively remove these biologically persistent TrOCs although the dynamic fouling layer formed on the MF membrane surface rejected them to some extent (Figure 7b). Nevertheless, the high rejection RO membrane complemented well to MBR for the high overall removal of these compounds.

3.3 Reverse osmosis membrane fouling

Water flux of the RO process subsequent to conventional MBR was adjusted daily to match that of the RO process subsequent to OMBR (Section 2.3). Changes in the applied hydraulic pressures to the RO membrane in these two hybrid systems are shown in Figure 8a. To compare fouling development on the RO membrane surface, the normalized water permeability was also determined (Figure 8b), which is the ratio of the effective membrane water permeability to the initial value (P/P_0).

[Figure 8]

The normalized water permeability of the RO membrane decreased less significantly than in conventional MBR-RO (Figure 8). This result indicates that the RO membrane fouling was more severe when treating conventional MBR effluent compared to reconcentrating the

528 OMBR draw solution due to their different water qualities and foulant contents (Figures 5
529 and 6). Thus, although the RO membrane in OMBR-RO was operated at a higher initial
530 hydraulic pressure to overcome the osmotic pressure of the draw solution (i.e. 0.5 M NaCl),
531 the hydraulic pressure applied to the RO membrane in conventional MBR-RO increased
532 much more rapidly and frequent RO membrane replacement was needed to match the water
533 flux of OMBR-RO (Figure 8a). Severe RO membrane fouling observed in conventional
534 MBR-RO can be attributed to foulant accumulation in the MBR effluent reservoir. Indeed,
535 EEM analysis revealed foulant build-up, such as humic-like ($\lambda_{ex/em}$=300-370/400-500 nm)
536 and protein-like substances ($\lambda_{ex/em}$=275-290/330-370 nm), in the MBR effluent (Figure S5,
537 Supplementary Data).

538 The FO process effectively prevented foulants from permeating into the draw solution
539 (Figures 6 and 7), thereby reducing membrane fouling in the downstream RO process. For
540 instance, the humic- and protein-like substances accumulated considerably in the bioreactor,
541 but their presence in the draw solution was negligible (Figure S5, Supplementary Data).
542 However, the RO normalized water permeability decreased gradually and stabilized at
543 approximately 0.35 from day 20 onward during OMBR-RO operation (Figure 8b). The
544 observed permeability decline could be attributed to membrane compaction (particularly
545 within the first week of operation) and fouling under the high hydraulic pressure (Figure 8a).

546 The fouling layer on the RO membrane surface exhibited different morphologies in OMBR-
547 RO and conventional MBR-RO (Figure 9a, b). Foulant clusters were sparsely distributed
548 without forming a dense fouling layer on the RO membrane surface subsequent to OMBR
549 (Figure 9a). Elementary analysis by EDS revealed that these clusters comprised carbon,
550 oxygen, sodium, and chloride (Figure 9c). By contrast, a compact and homogenous cake
551 layer formed on the RO membrane surface in conventional MBR-RO (Figure 9b),
552 predominantly containing carbon, oxygen, magnesium, calcium, and phosphate (Figure 9d).

553 This result indicates the formation of both organic and inorganic membrane fouling. However,
554 regularly shaped or needle-like crystals typically formed with inorganic scaling were not
555 visualized on the RO membrane surface subsequent to conventional MBR although
556 magnesium, calcium, and phosphate were detected (Figure 9b). This result was possibly due
557 to the formation of inorganic precipitates in the organic fouling layer or the complexation
558 between these divalent cations and organic molecules (e.g. protein-like substances) on the
559 membrane surface (Zhao et al., 2010).

560 **[Figure 9]**

561 Organic fouling layer on the RO membrane surface was characterized by ATR-FTIR
562 measurement (Figure 10). The pristine RO membrane showed typical absorbance peaks at
563 wavenumbers of 3345 cm^{-1} (N-H stretching), 3300 cm^{-1} (O-H stretching), 1671 cm^{-1} (strong
564 amide C=O), 2946 and 1487cm^{-1} (C-H stretching), and 1168 cm^{-1} (amide ring). Similar ATR-
565 FTIR spectra were also observed for the RO membrane coupled with OMBR, confirming the
566 formation of slight and scattered organic fouling layer on the membrane surface. By contrast,
567 the RO membrane subsequent to conventional MBR exhibited distinctive adsorption peaks at
568 1653 cm^{-1}, which usually associates with alkene (C=C) in aliphatic structures and/or amide I
569 (C=O) bonds, and at 1543 cm^{-1}, representing amide II (C-N-H) bonds. In addition, the fouled
570 RO membrane also showed a sharp peak at 1032 cm^{-1}, indicating carbonyl (C=O) bonds of
571 polysaccharides. These results suggest that humic- and protein-like substances accumulated
572 in the MBR effluent were likely responsible for the severe organic fouling of the RO
573 membrane in conventional MBR-RO.

574 **[Figure 10]**

3.4 Implications

High product water quality and low membrane fouling imply robustness of OMBR-RO in advanced wastewater treatment and water reuse. Results reported here highlight the benefits of OMBR-RO over conventional MBR-RO. Compared to conventional MBR-RO, the high rejection FO membrane prevents the downstream RO process from severe membrane fouling, thereby reducing membrane cleaning and maintenance during OMBR-RO operation. Moreover, OMBR-RO has the potential to simultaneously achieve seawater desalination and wastewater recycling when seawater is used as the draw solution in coastal regions. By virtue of osmotic dilution, low pressure RO systems can be coupled with OMBR to remove the need for concentrate disposal, thereby reducing energy consumption for seawater desalination and wastewater recovery (Valladares Linares et al., 2016). several strategies to mitigate salinity build-up in OMBR have been proposed, for example, by using organic draw solutions (Luo et al., 2016a) and integrating with the MF/UF membrane for salt bleeding (Holloway et al., 2015; Luo et al., 2016b).

Sludge produced by OMBR is expected to be saline. Thus, further study is necessary to quantify the impact of salinity on subsequent sludge treatment and available sludge reuse options.

4. Conclusion

Results reported here show that both OMBR-RO and conventional MBR-RO systems can effectively remove bulk organic matter, nutrients, and all 31 TrOCs investigated. Nevertheless, salinity build-up in the bioreactor reduced the water flux and adversely impacted biological stability by altering biomass characteristics and microbial community structure during OMBR operation. Salinity increase also resulted in more SMP and EPS in the mixed liquor, inducing the FO membrane fouling. With the succession of halophobic

599 bacteria by halotolerant ones, the OMBR system remained biologically active. Moreover, the
600 high rejection of foulants by the FO membrane prevented the downstream RO process from
601 severe membrane fouling. In contrast to biological variation in OMBR, biological
602 performance was relatively stable during conventional MBR operation. However, foulants
603 (e.g. humic- and protein-like matters and inorganic salts) accumulated considerably in the
604 MBR effluent reservoir, resulting in severe fouling to the subsequent RO membrane.

605 ## 5. References

606 Achilli, A., Cath, T.Y., Marchand, E.A., Childress, A.E., 2009. The forward osmosis
607 membrane bioreactor: A low fouling alternative to MBR processes. Desalination 239, 10-
608 21.

609 Al Ashhab, A., Herzberg, M., Gillor, O., 2014. Biofouling of reverse-osmosis membranes
610 during tertiary wastewater desalination: Microbial community composition. Water Res.
611 50, 341-349.

612 Alturki, A.A., McDonald, J., Khan, S.J., Hai, F.I., Price, W.E., Nghiem, L.D., 2012.
613 Performance of a novel osmotic membrane bioreactor (OMBR) system: Flux stability and
614 removal of trace organics. Bioresour. Technol. 113, 201-206.

615 Alturki, A.A., McDonald, J.A., Khan, S.J., Price, W.E., Nghiem, L.D., Elimelech, M., 2013.
616 Removal of trace organic contaminants by the forward osmosis process. Sep. Purif.
617 Technol. 103, 258-266.

618 Alturki, A.A., Tadkaew, N., McDonald, J.A., Khan, S.J., Price, W.E., Nghiem, L.D., 2010.
619 Combining MBR and NF/RO membrane filtration for the removal of trace organics in
620 indirect potable water reuse applications. J. Membr. Sci. 365, 206-215.

621 APHA. 2005. Standard methods for the examination of water and wastewater. APHA-
622 AWWA-WEF. 9780875530475, 0875530478.

623 Caporaso, J.G., Kuczynski, J., Stombaugh, J., Bittinger, K., Bushman, F.D., Costello, E.K.,
624 Fierer, N., Peña, A.G., Goodrich, J.K., Gordon, J.I., Huttley, G.A., Kelley, S.T., Knights,
625 D., Koenig, J.E., Ley, R.E., Lozupone, C.A., McDonald, D., Muegge, B.D., Pirrung, M.,
626 Reeder, J., Sevinsky, J.R., Turnbaugh, P.J., Walters, W.A., Widmann, J., Yatsunenko, T.,
627 Zaneveld, J., Knight, R., 2010. QIIME allows analysis of high-throughput community
628 sequencing data. Nat. Methods 7, 335-336.
629 Cath, T.Y., Hancock, N.T., Lampi, J., Nghiem, L.D., Xie, M., Yip, N.Y., Elimelech, M.,
630 McCutcheon, J.R., McGinnis, R.L., Achilli, A., Anastasio, D., Brady, A.R., Childress,
631 A.E., Farr, I.V., 2013. Standard methodology for evaluating membrane performance in
632 osmotically driven membrane processes. Desalination 312, 31-38.
633 Chen, L., Gu, Y., Cao, C., Zhang, J., Ng, J.-W., Tang, C., 2014. Performance of a submerged
634 anaerobic membrane bioreactor with forward osmosis membrane for low-strength
635 wastewater treatment. Water Res. 50, 114-123.
636 Clara, M., Strenn, B., Gans, O., Martinez, E., Kreuzinger, N., Kroiss, H., 2005. Removal of
637 selected pharmaceuticals, fragrances and endocrine disrupting compounds in a membrane
638 bioreactor and conventional wastewater treatment plants. Water Res. 39, 4797-4807.
639 Cornelissen, E.R., Harmsen, D., Beerendonk, E.F., Qin, J.J., Oo, H., De Korte, K.F.,
640 Kappelhof, J.W.M.N., 2011. The innovative osmotic membrane bioreactor (OMBR) for
641 reuse of wastewater. Water Sci. Technol. 63, 1557-1565.
642 Cory, R.M., McKnight, D.M., 2005. Fluorescence spectroscopy reveals ubiquitous presence
643 of oxidized and reduced quinones in dissolved organic matter. Environ. Sci. Technol. 39,
644 8142-8149.
645 D'Haese, A., Le-Clech, P., Van Nevel, S., Verbeken, K., Cornelissen, E.R., Khan, S.J.,
646 Verliefde, A.R.D., 2013. Trace organic solutes in closed-loop forward osmosis

applications: Influence of membrane fouling and modeling of solute build-up. Water Res. 47, 5232-5244.

De Wever, H., Weiss, S., Reemtsma, T., Vereecken, J., Müller, J., Knepper, T., Rörden, O., Gonzalez, S., Barcelo, D., Dolores Hernando, M., 2007. Comparison of sulfonated and other micropollutants removal in membrane bioreactor and conventional wastewater treatment. Water Res. 41, 935-945.

Edgar, R.C., 2013. UPARSE: Highly accurate OTU sequences from microbial amplicon reads. Nat. Methods 10, 996-998.

Elimelech, M., Phillip, W.A., 2011. The future of seawater desalination: Energy, technology, and the environment. Science 333, 712-717.

Fane, A.G., Wang, R., Hu, M.X., 2015. Synthetic Membranes for Water Purification: Status and Future. Angew. Chem. Int. Ed.

Farias, E.L., Howe, K.J., Thomson, B.M., 2014. Effect of membrane bioreactor solids retention time on reverse osmosis membrane fouling for wastewater reuse. Water Res. 49, 53-61.

Gerrity, D., Pecson, B., Trussell, R.S., Trussell, R.R., 2013. Potable reuse treatment trains throughout the world. J. Water Supply Res. Technol. AQUA 62, 321-338.

Hai, F.I., Tessmer, K., Nguyen, L.N., Kang, J., Price, W.E., Nghiem, L.D., 2011. Removal of micropollutants by membrane bioreactor under temperature variation. J. Membr. Sci. 383, 144-151.

Hai, F.I., Yamamoto, K., Lee, C.H. 2014. Membrane Biological Reactors: Theory, Modeling, Design, Management and Applications to Wastewater Reuse. IWA Publishing, London.

Hancock, N.T., Xu, P., Heil, D.M., Bellona, C., Cath, T.Y., 2011. Comprehensive bench- and pilot-scale investigation of trace organic compounds rejection by forward osmosis. Environ. Sci. Technol. 45, 8483-8490.

672 Henderson, R.K., Baker, A., Murphy, K.R., Hambly, A., Stuetz, R.M., Khan, S.J., 2009.
673 Fluorescence as a potential monitoring tool for recycled water systems: A review. Water
674 Research 43, 863-881.
675 Holloway, R.W., Childress, A.E., Dennett, K.E., Cath, T.Y., 2007. Forward osmosis for
676 concentration of anaerobic digester centrate. Water Res. 41, 4005-4014.
677 Holloway, R.W., Regnery, J., Nghiem, L.D., Cath, T.Y., 2014. Removal of trace organic
678 chemicals and performance of a novel hybrid ultrafiltration-osmotic membrane
679 bioreactor. Environ. Sci. Technol. 48, 10859-10868.
680 Holloway, R.W., Wait, A.S., Da Silva, A.F., Herron, J., Schutter, M.D., Lampi, K., Cath,
681 T.Y., 2015. Long-term pilot scale investigation of novel hybrid ultrafiltration-osmotic
682 membrane bioreactors. Desalination 363, 64.
683 Kim, Y., Elimelech, M., Shon, H.K., Hong, S., 2014. Combined organic and colloidal fouling
684 in forward osmosis: Fouling reversibility and the role of applied pressure. J. Membr. Sci.
685 460, 206-212.
686 Lay, W.C.L., Liu, Y., Fane, A.G., 2010. Impacts of salinity on the performance of high
687 retention membrane bioreactors for water reclamation: A review. Water Res. 44, 21-40.
688 Lu, X., Ma, J., Nejati, S., Choo, Y., Osuji, C.O., Elimelech, M., 2015. Elements provide a
689 clue: Nanoscale characterization of thin-film composite polyamide membranes. ACS
690 Appl. Mater. Interfaces 7, 16917-16922.
691 Luo, W., Hai, F.I., Price, W.E., Elimelech, M., Nghiem, L.D., 2016a. Evaluating ionic
692 organic draw solutes in osmotic membrane bioreactors for water reuse. J. Membr. Sci.
693 514, 636-645.
694 Luo, W., Hai, F.I., Price, W.E., Guo, W., Ngo, H.H., Yamamoto, K., Nghiem, L.D., 2014a.
695 High retention membrane bioreactors: Challenges and opportunities. Bioresour. Technol.
696 167, 539-546.

Luo, W., Hai, F.I., Price, W.E., Guo, W., Ngo, H.H., Yamamoto, K., Nghiem, L.D., 2016b. Phosphorus and water recovery by a novel osmotic membrane bioreactor–reverse osmosis system. Bioresour. Technol. 200, 297-304.

Luo, W., Hai, F.I., Price, W.E., Nghiem, L.D., 2015a. Water extraction from mixed liquor of an aerobic bioreactor by forward osmosis: Membrane fouling and biomass characteristics assessment. Sep. Purif. Technol. 145, 56-62.

Luo, W., Phan, H.V., Hai, F.I., Price, W.E., Guo, W., Ngo, H.H., Yamamoto, K., Nghiem, L.D., 2016c. Effects of salinity build-up on the performance and bacterial community structure of a membrane bioreactor. Bioresour. Technol. 200, 305-310.

Luo, W.H., Hai, F.I., Kang, J.G., Price, W.E., Guo, W.S., Ngo, H.H., Yamamoto, K., Nghiem, L.D., 2015b. Effects of salinity build-up on biomass characteristics and trace organic chemical removal: Implications on the development of high retention membrane bioreactors. Bioresour. Technol. 177, 274-281.

Luo, Y.L., Guo, W.S., Ngo, H.H., Nghiem, L.D., Hai, F.I., Zhang, J., Liang, S., Wang, X.C.C., 2014b. A review on the occurrence of micropollutants in the aquatic environment and their fate and removal during wastewater treatment. Sci. Total Environ. 473, 619-641.

Mi, B., Elimelech, M., 2010. Organic fouling of forward osmosis membranes: Fouling reversibility and cleaning without chemical reagents. J. Membr. Sci. 348, 337-345.

Nghiem, L.D., Coleman, P.J., 2008. NF/RO filtration of the hydrophobic ionogenic compound triclosan: Transport mechanisms and the influence of membrane fouling. Sep. Purif. Technol. 62, 709-716.

Nguyen, L.N., Hai, F.I., Kang, J., Price, W.E., Nghiem, L.D., 2013. Removal of emerging trace organic contaminants by MBR-based hybrid treatment processes. Int. Biodeterior. Biodegrad. 85, 474-482.

721 Nguyen, N.C., Chen, S.-S., Nguyen, H.T., Ray, S.S., Ngo, H.H., Guo, W., Lin, P.-H., 2016.
722 Innovative sponge-based moving bed–osmotic membrane bioreactor hybrid system using
723 a new class of draw solution for municipal wastewater treatment. Water Res. 91, 305-313.
724 Phan, H.V., Hai, F.I., Zhang, R., Kang, J., Price, W.E., Nghiem, L.D., 2016. Bacterial
725 community dynamics in an anoxic-aerobic membrane bioreactor – Impact on nutrient and
726 trace organic contaminant removal. Int. Biodeterior. Biodegrad. 109, 61-72.
727 Semblante, G.U., Hai, F.I., Bustamante, H., Guevara, N., Price, W.E., Nghiem, L.D., 2015.
728 Effects of iron salt addition on biosolids reduction by oxic-settling-anoxic (OSA) process.
729 Int. Biodeterior. Biodegrad. 104, 391-400.
730 Shaffer, D.L., Werber, J.R., Jaramillo, H., Lin, S., Elimelech, M., 2015. Forward osmosis:
731 Where are we now? Desalination 356, 271-284.
732 Shaffer, D.L., Yip, N.Y., Gilron, J., Elimelech, M., 2012. Seawater desalination for
733 agriculture by integrated forward and reverse osmosis: Improved product water quality for
734 potentially less energy. J. Membr. Sci. 415-416, 1-8.
735 Tadkaew, N., Hai, F.I., McDonald, J.A., Khan, S.J., Nghiem, L.D., 2011. Removal of trace
736 organics by MBR treatment: The role of molecular properties. Water Res. 45, 2439-2451.
737 Tian, M., Wang, Y.-N., Wang, R., 2015. Synthesis and characterization of novel high-
738 performance thin film nanocomposite (TFN) FO membranes with nanofibrous substrate
739 reinforced by functionalized carbon nanotubes. Desalination 370, 79-86.
740 Valladares Linares, R., Li, Z., Yangali-Quintanilla, V., Ghaffour, N., Amy, G., Leiknes, T.,
741 Vrouwenvelder, J.S., 2016. Life cycle cost of a hybrid forward osmosis – low pressure
742 reverse osmosis system for seawater desalination and wastewater recovery. Water Res.
743 88, 225-234.

744 Wang, X.H., Yuan, B., Chen, Y., Li, X.F., Ren, Y.P., 2014. Integration of micro-filtration
745 into osmotic membrane bioreactors to prevent salinity build-up. Bioresour. Technol. 167,
746 116-123.
747 Wei, R., Zhang, S., Cui, Y., Ong, R.C., Chung, T.-S., Helmer, B.J., de Wit, J.S., 2015. Highly
748 permeable forward osmosis (FO) membranes for high osmotic pressure but viscous draw
749 solutes. J. Membr. Sci. 496, 132-141.
750 Werber, J.R., Osuji, C.O., Elimelech, M., 2016. Materials for next-generation desalination
751 and water purification membranes. Nat. Rev. Mater. 1, 16018.
752 Wijekoon, K.C., Hai, F.I., Kang, J., Price, W.E., Guo, W., Ngo, H.H., Nghiem, L.D., 2013.
753 The fate of pharmaceuticals, steroid hormones, phytoestrogens, UV-filters and pesticides
754 during MBR treatment. Bioresour. Technol. 144, 247-254.
755 Wu, B., Kitade, T., Chong, T.H., Lee, J.Y., Uemura, T., Fane, A.G., 2013. Flux-dependent
756 fouling phenomena in membrane bioreactors under different food to microorganisms
757 (F/M) ratios. Sep. Sci. Technol. 48, 840-848.
758 Xie, M., Gray, S.R., 2016. Transport and accumulation of organic matter in forward osmosis-
759 reverse osmosis hybrid system: Mechanism and implications. Sep. Purif. Technol. 167, 6-
760 16.
761 Xie, M., Lee, J., Elimelech, M., Nghiem, L.D., 2015. Role of pressure in organic fouling in
762 forward osmosis and reverse osmosis. J. Membr. Sci. 493, 748-754.
763 Xie, M., Nghiem, L.D., Price, W.E., Elimelech, M., 2014. Relating rejection of trace organic
764 contaminants to membrane properties in forward osmosis: Measurements, modelling and
765 implications. Water Res. 49, 265-274.
766 Yogalakshmi, K.N., 2010. Effect of transient sodium chloride shock loads on the
767 performance of submerged membrane bioreactor. Bioresour. Technol. 101, 7054-7061.

768 Zhang, J.J., Kobert, K., Flouri, T., Stamatakis, A., 2014. PEAR: a fast and accurate Illumina
769 Paired-End reAd mergeR. Bioinformatics 30, 614-620.
770 Zhang, L., Gao, G., Tang, X., Shao, K., Bayartu, S., Dai, J., 2013. Bacterial community
771 changes along a salinity gradient in a Chinese wetland. Can. J. Microbiol. 59, 611-619.
772 Zhang, X., Bishop, P.L., Kinkle, B.K., 1999. Comparison of extraction methods for
773 quantifying extracellular polymers in biofilms. Water Sci. Technol. 39, 211-218.
774 Zhao, Y., Song, L., Ong, S.L., 2010. Fouling behavior and foulant characteristics of reverse
775 osmosis membranes for treated secondary effluent reclamation. J. Membr. Sci. 349, 65-
776 74.

LIST OF FIGURES

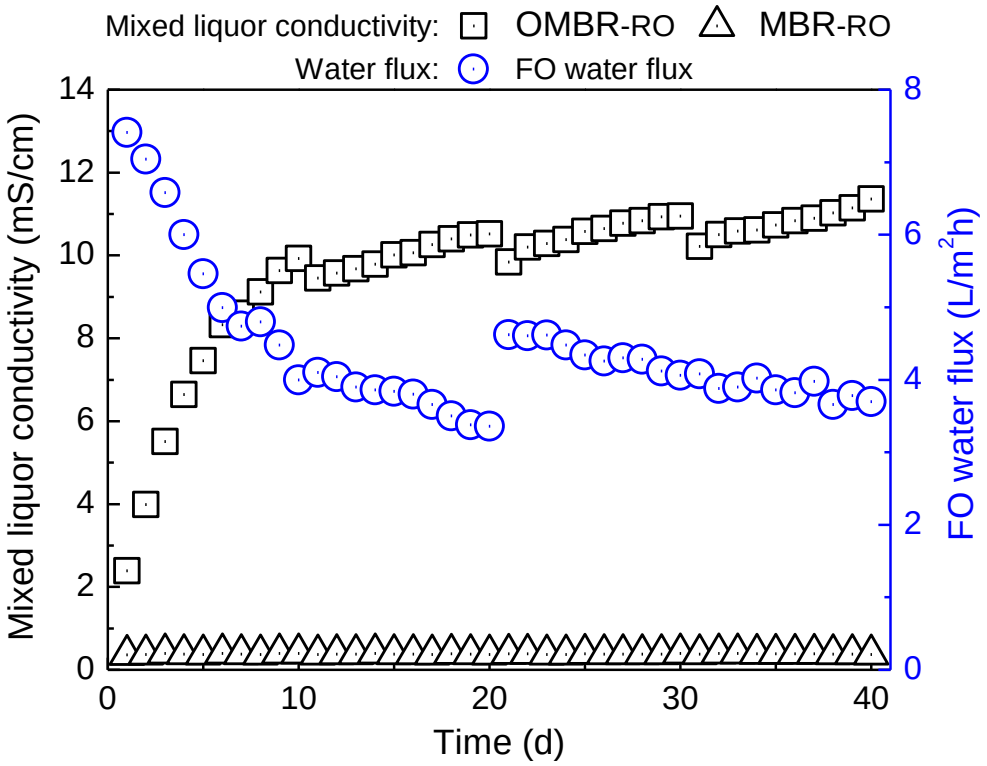

Figure 1: Mixed liquor electrical conductivity and FO water flux during OMBR-RO and conventional MBR-RO operation. MF (used in conventional MBR) and RO water fluxes were adjusted daily to match that of FO. The MF membrane was operated in a cycle of 14 min on and 1 min off. Experimental conditions: DO = 5 mg/L; initial MLSS = 5.5 g/L; HRT = 27 – 60 h; SRT = 20 d; temperature = 22 ± 1 ºC; initial FO draw solution = 0.5 M NaCl; draw cross-flow velocity = 2.8 cm/s; RO cross-flow velocity = 41.5 cm/s. On day 20, 100 g NaCl was added to OMBR draw solution (with constant working volume of 10 L) to replenish draw solute loss.

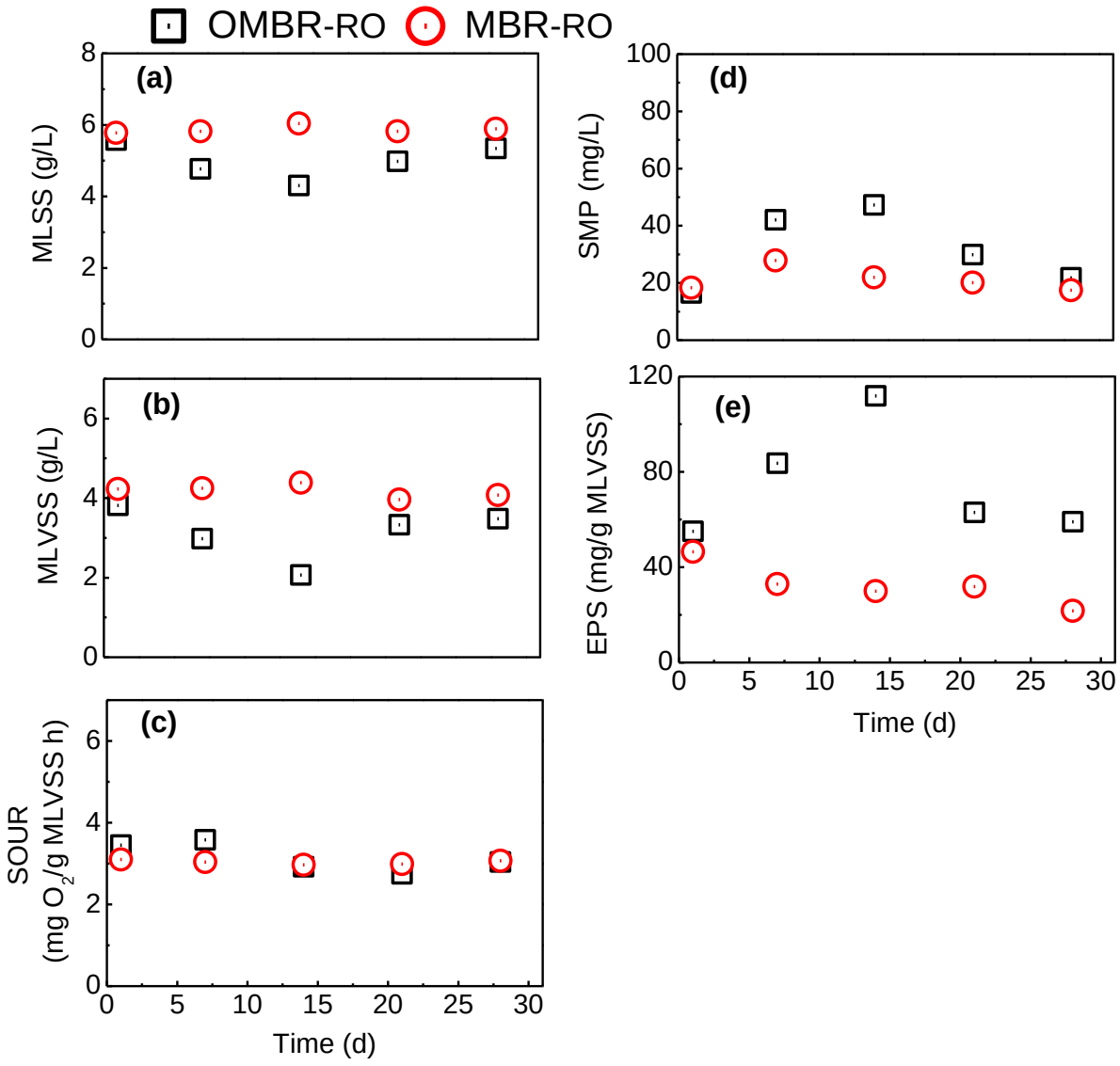

787

788 **Figure 2:** Key biomass characteristics during OMBR-RO and conventional MBR-RO
789 operation.

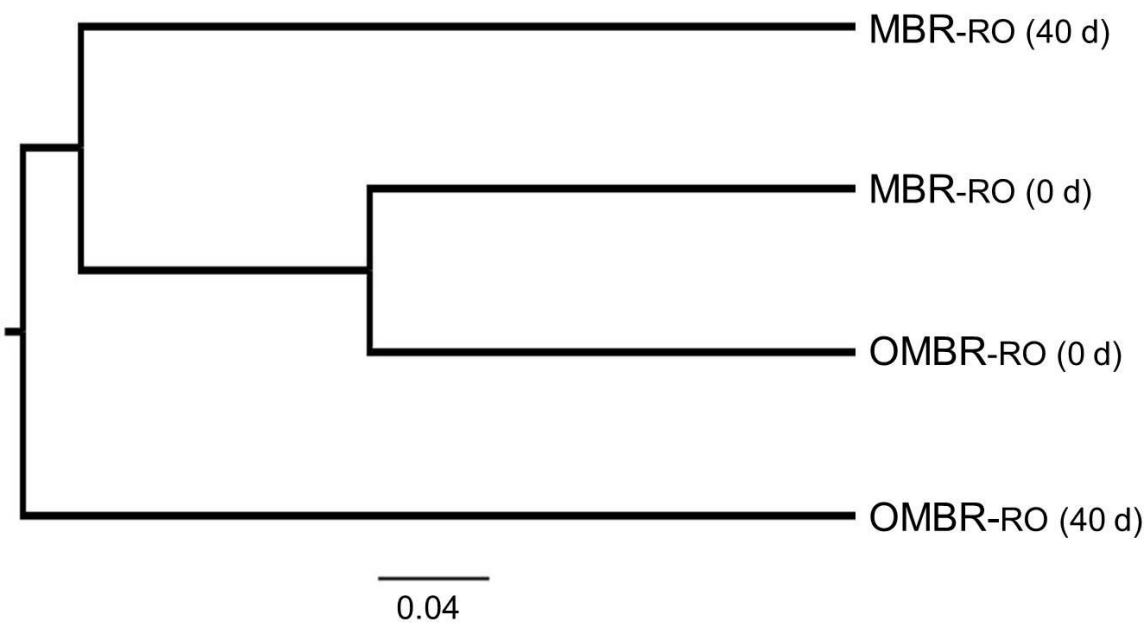

790

791 **Figure 3:** Hierarchical clustering based on the unweighted UniFrac metric. The branch length
792 represents the distance (indicated by scale bar) among bacterial communities of sludge
793 samples in UniFrac units. Labels on the branch indicate sludge samples collected from
794 bioreactors at the beginning (0 day) and conclusion (40 day) of OMBR-RO and conventional
795 MBR-RO operation. Experimental conditions are as described in the caption of Figure 1.

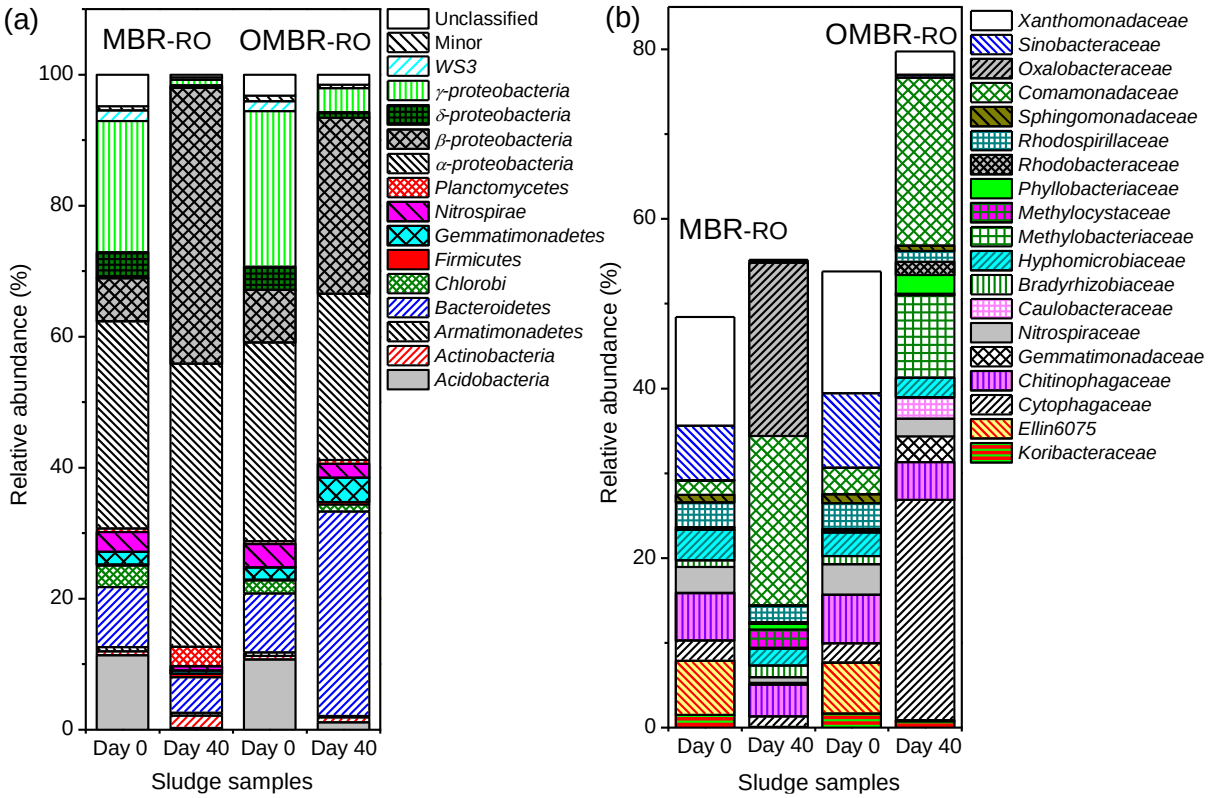

Figure 4: Relative abundance of dominant (a) phyla and (b) families (>1%) in sludge samples collected from bioreactors at the beginning (day 0) and conclusion (day 40) of OMBR-RO and conventional MBR-RO operation. The phylum *Proteobacteria* comprised the classes *α*-, *β*-, *δ*- and *γ-proteobacteria*. Phyla with relative abundance < 0.5% were grouped as "Minor".

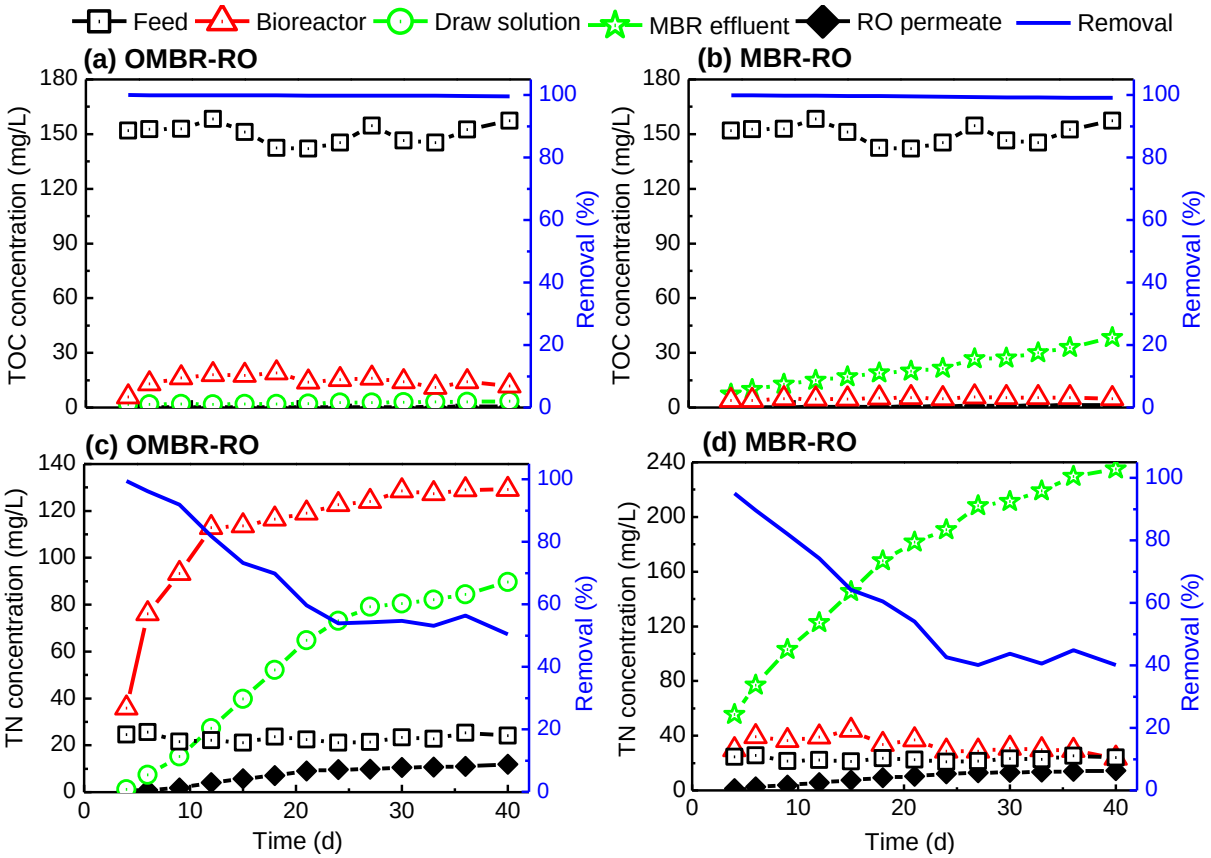

Figure 5: TOC and TN concentrations and removal rates during OMBR-RO and conventional MBR-RO operation. The two systems were operated under the same conditions as described in the caption of Figure 1.

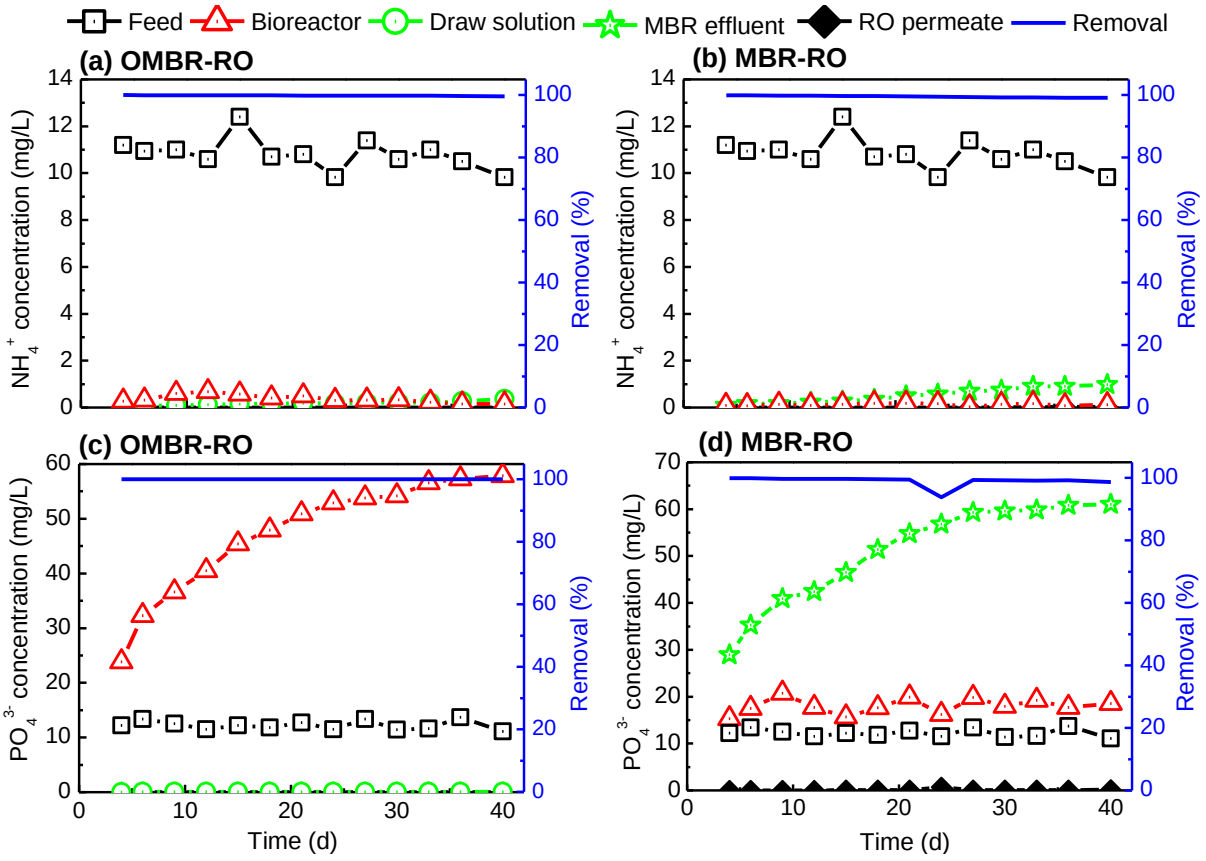

Figure 6: NH_4^+ and PO_4^{3-} concentrations and removal rates during OMBR-RO and conventional MBR-RO operation. Experimental conditions are as described in the caption of Figure 1.

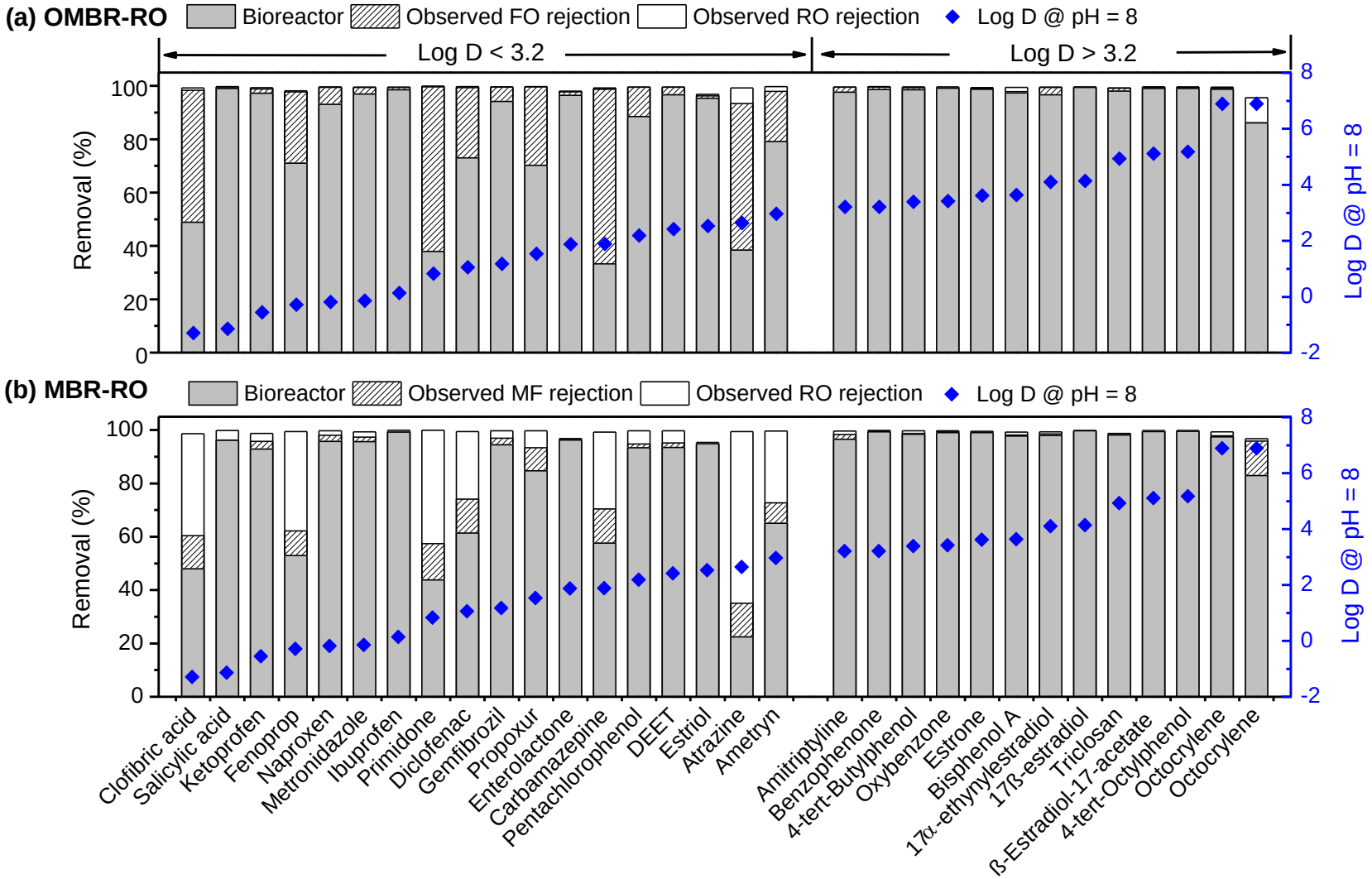

812

813 **Figure 7:** TrOC removal by different compartments of (a) OMBR-RO and (b) conventional MBR-RO. Average removal data obtained from four

814 measurements (once every ten days) were demonstrated with standard deviation in the range of 0 – 20% (not shown in the Figure). Based on

their effective octanol-water partition coefficient (Log D) at solution pH 8, the 30 TrOCs investigated were classified as hydrophobic (i.e. Log D > 3.2) and hydrophilic (i.e. Log D < 3.2). Observed TrOC rejection rates do not reflect the real separation capacity of the membranes, but can be used to infer their contributions to TrOC removal in the two hybrid systems. Experimental conditions are as described in the caption of Figure 1.

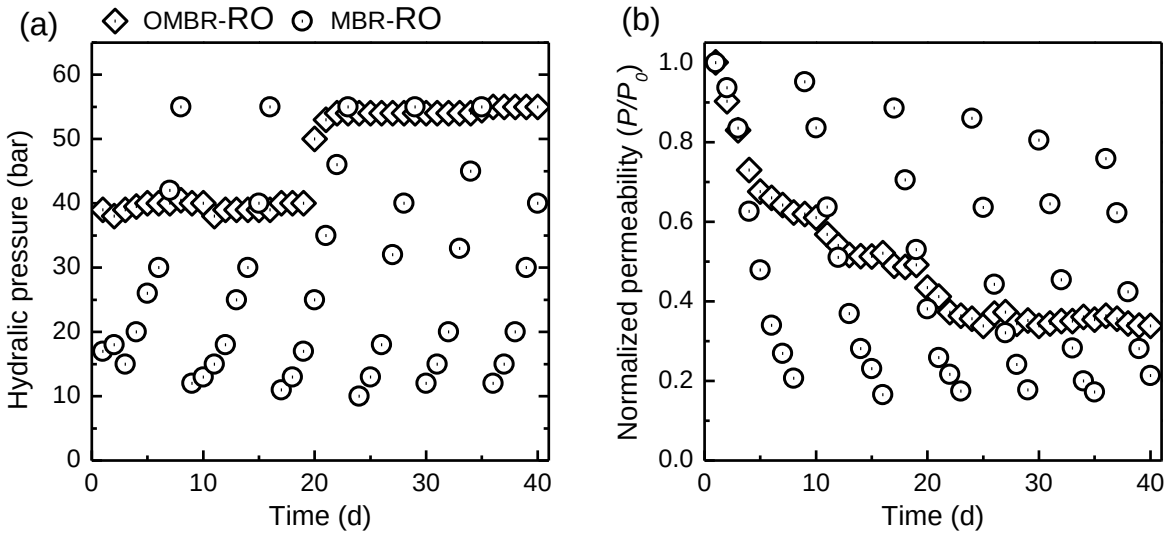

Figure 8: Hydraulic pressure (a) applied to the RO membrane and its normalized permeability (b) during OMBR-RO and conventional MBR-RO operation. The normalized water permeability was the ratio of the effective membrane water permeability to the initial value (P/P_0). Water flux of the RO membranes was adjusted daily to match that of OMBR. On day 20, 100 g NaCl was added to OMBR draw solution (with constant working volume of 10 L) to replenish draw solute loss. A new RO membrane was used once the membrane normalized permeability decreased to 0.2. Experimental conditions are as described in the caption of Figure 1.

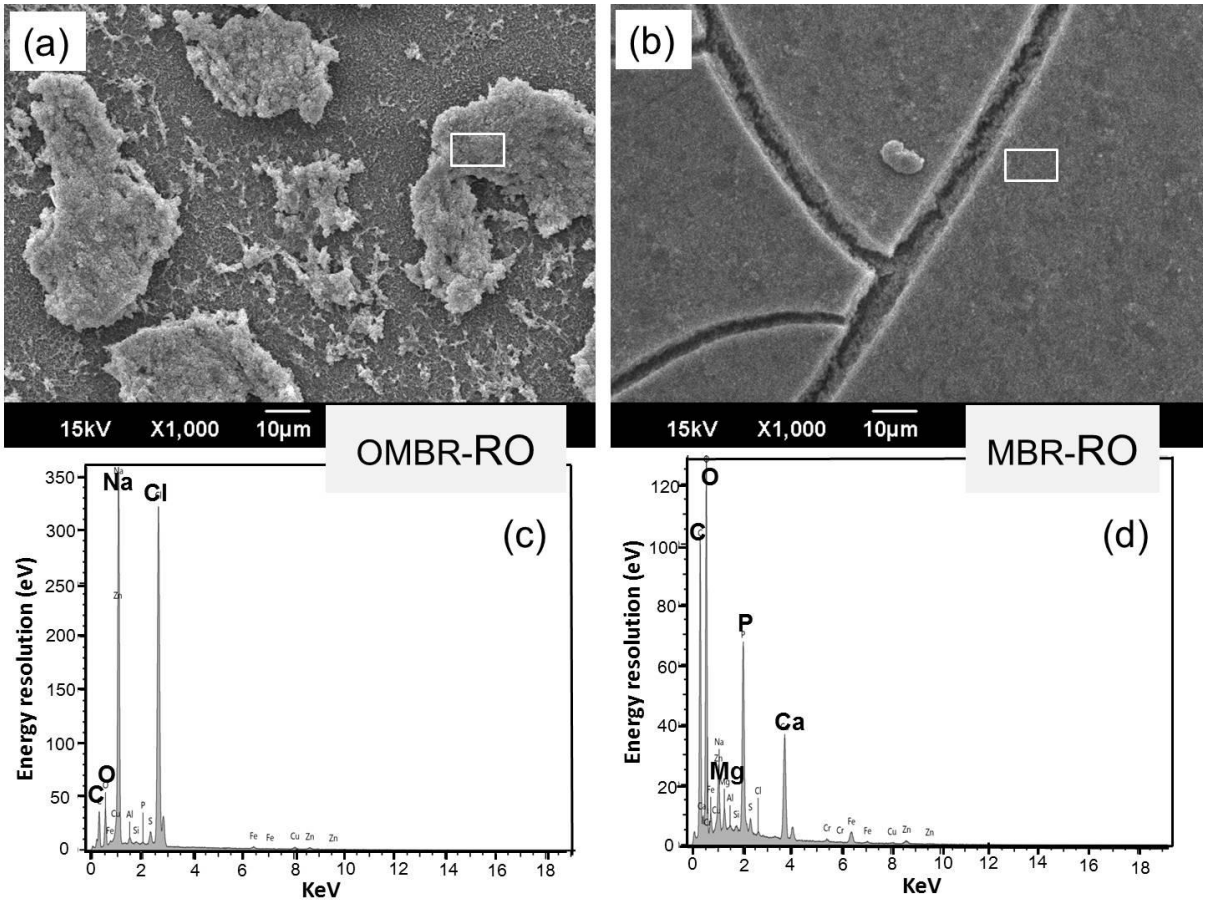

827

828 **Figure 9:** (a, b) SEM and (c, d) EDS analyses of the RO membrane surfaces at the
829 conclusion of OMBR-RO and conventional MBR-RO operation. Experimental conditions
830 were as described in the caption of Figure 1.

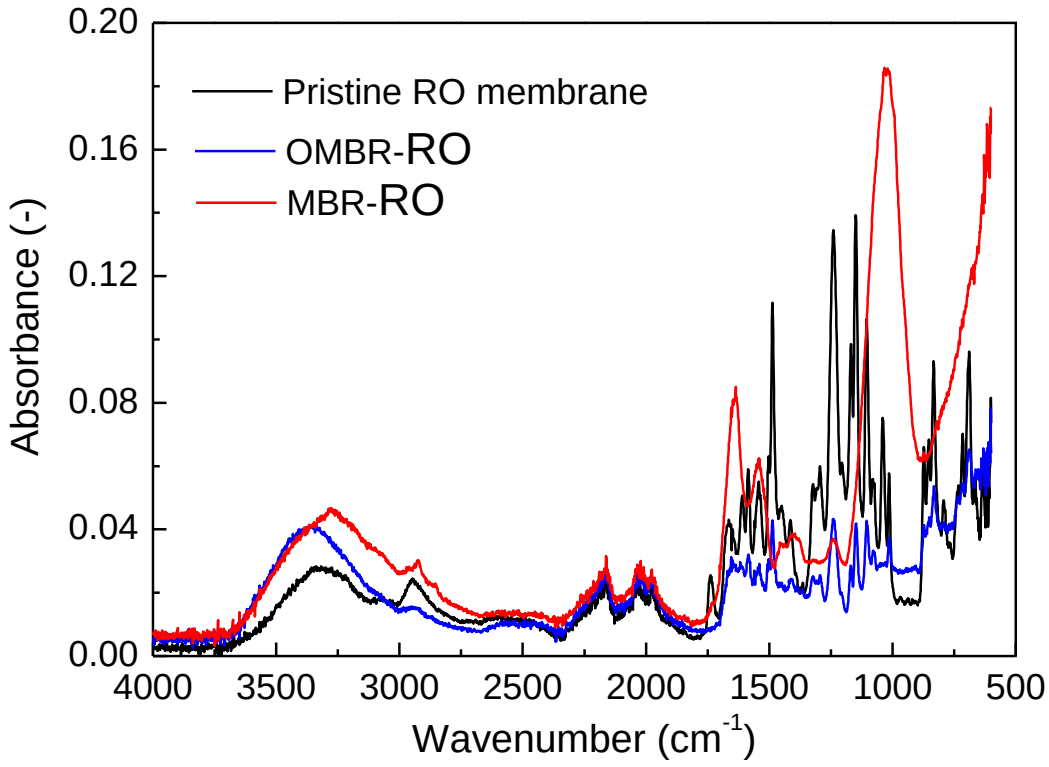

831

832 **Figure 10:** ATR-FTIR absorption spectra of the RO membrane surfaces before and after
833 OMBR-RO and conventional MBR-RO operation. Experimental conditions are as described
834 in the caption of Figure 1.

835